# On the Pareto Set and Front of Multiobjective Spherical Functions with Convex Constraints

Anne Auger
Dimo Brockhoff
firstname.lastname@inria.fr
Inria, CMAP, CNRS, École Polytechnique, Institut Polytechnique de Paris
Palaiseau, France

Jordan N. Cork
Tea Tušar
firstname.lastname@ijs.si
Jožef Stefan Institute and Jožef Stefan International Postgraduate School
Ljubljana, Slovenia

## ABSTRACT

We analyze a fundamental class of multiobjective constrained problems where the objectives are spherical functions and the constraints are convex. As an application from the projection theorem on closed convex sets, we prove that the constrained Pareto set corresponds to the orthogonal projection of the unconstrained Pareto set onto the feasible region. We establish this fundamental geometric property and illustrate its implications using visualizations of Pareto sets and fronts under various constraint configurations. Furthermore, we assess the performance of NSGA-II on these problems, examining its ability to approximate the constrained Pareto set across different dimensions. Our findings highlight the importance of theoretically grounded and understood benchmark problems for assessing algorithmic behavior and contribute to a deeper understanding of constrained multiobjective landscapes.

## CCS CONCEPTS

• **Mathematics of computing** → **Continuous functions**; **Continuous optimization**; • **Computing methodologies** → **Continuous space search**; • **Applied computing** → **Multi-criterion optimization and decision-making**.

## KEYWORDS

multiobjective constrained optimization, benchmarking, test functions

**ACM Reference Format:**
Anne Auger, Dimo Brockhoff, Jordan N. Cork, and Tea Tušar. 2025. On the Pareto Set and Front of Multiobjective Spherical Functions with Convex Constraints. In *Genetic and Evolutionary Computation Conference (GECCO '25), July 14–18, 2025, Malaga, Spain.* ACM, New York, NY, USA, 9 pages. https://doi.org/10.1145/3712256.3726432

## 1 INTRODUCTION

Many real-world optimization problems have multiple objectives as well as constraints. It is therefore important to design algorithms that can handle both. To achieve this, we need appropriate test problems that allow us to assess algorithm performance—specifically, whether they converge to the set of optimal solutions, how quickly they do so, and whether they respect the given constraints.

Several test suites with constrained multiobjective problems have been proposed in the past, see [11] for a recent review. To the best of our knowledge, however, they all have constraints of one of two types: either 1) constraints on the objective space with a well identified impact only on the Pareto front, while the impact on the Pareto set is typically unclear [11, for almost all mentioned suites] or 2) very specific constraints in the search space that do not affect the Pareto set [6, 12, 15, 18]. Moreover, a recent study showed experimentally that the inspected real-world constrained multiobjective problems do not possess constraints of the first type. Consequently, selected constrained multiobjective optimizers performed differently on the real-world problems than on the test problems stemming from those suites [13].

In the case of single-objective optimization, on the contrary, established benchmark suites are usually defined around problem properties observed in practice such as ill-conditioning, non-separability, multi-modality, etc. [7]. Convex-quadratic functions constitute an important class of single-objective functions that model the landscape of the problem in the neighborhood of one optimum including instances with ill-conditioned Hessian, a difficulty frequently encountered on real-world problems that any well-designed algorithm should be able to address. Those functions are well understood and constitute a very useful class of problems for designing algorithms for non-linear and non-quadratic problems.

A similar approach to designing test functions in the unconstrained multiobjective case is to combine (simple) single-objective functions and thus the difficulties of single-objective problems. Such an approach is not new [9, 16] and has been used also when defining the `bbob-biobj` test suite of the COCO platform [4, 7].

In this context, we argue that constrained multiobjective test problems should be comprehensible, capturing the difficulties an algorithm has to face when optimizing a real-world problem and with ideally a well-identified and well understood Pareto set that enables to diagnose and measure convergence. They should particularly include both well-conditioned and ill-conditioned problems, as well as simple linear constraints. Surprisingly, however, it seems that even the simplest multiobjective problems that model the landscape of a well-conditioned problem in the neighborhood of the optimum with linear constraints are not yet sufficiently understood.

Consider indeed for instance the bi-objective problem involving two spheres $f_1 : x \mapsto \frac{1}{2}\|x - c_1\|^2$ and $f_2 : x \mapsto \frac{1}{2}\|x - c_2\|^2$ for $c_1, c_2 \in \mathbb{R}^n$ with $c_1 \neq c_2$. Its Pareto set corresponds to the segment between $c_1$ and $c_2$ and can thus be expressed as

$$\mathrm{PS}^u = \{x_t = tc_1 + (1-t)c_2, t \in [0,1]\}. \quad (1)$$


*GECCO '25, July 14–18, 2025, Malaga, Spain*

ACM ISBN 979-8-4007-1465-8/2025/07
https://doi.org/10.1145/3712256.3726432

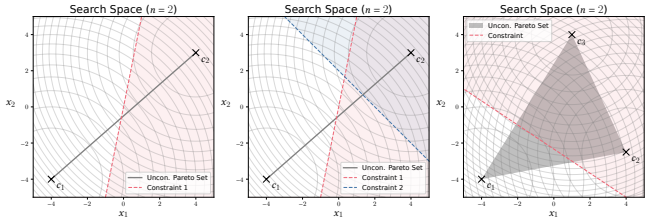


**Figure 1: Examples of 2-sphere and 3-sphere multiobjective problems with two variables. The optima of the single-objective functions are in $c_1$, $c_2$ and $c_3$. The Pareto sets are the segment $[c_1, c_2]$ in the left and middle plots and the convex hull of $\{c_1, c_2, c_3\}$ (i.e., the triangle with $c_1$, $c_2$ and $c_3$ as vertices) in the right plot. They are depicted in gray. Linear constraints are depicted in blue and red. The feasible set corresponds to the white area and its boundary.**

How does this Pareto set change when constraints are introduced? Consider the simplest case of a single linear constraint (see Figure 1, left). What form does the set of optimal solutions take in this constrained scenario? What if we add a second constraint (see Figure 1, middle)?

More generally, consider the $m$-sphere problem with different linear constraints (see Figure 1, right for $m = 3$). How does the Pareto set evolve in the presence of constraints? Interestingly, those seemingly straightforward questions remain largely unexplored, while they seem to be the most basic to have answered prior to testing whether a new algorithm converges towards the solution set of the problem it is optimizing.

In this context, we examine the $m$-sphere problem with $m$ convex inequality constraints and linear equality constraints. Building on classical results from convex optimization, we prove that the Pareto set of the constrained problem is the projection of the unconstrained Pareto set onto the feasible set. We finish with an illustration of how NSGA-II works on a specific case of these "simple" functions (including the effect of the search space dimension in terms of the achieved hypervolume indicator values).

The paper is further organized as follows: In Section 2, we present the problem setting and main result. In Section 3, we present the proof of our main result after introducing the different mathematical tools needed. In Section 4, as an application, we show how NSGA-II approaches the Pareto optimal set on a simple multiobjective problem with linear constraints.

*Notations.* In the entire paper, for $x \in \mathbb{R}^n$, $\|x\|$ denotes its Euclidean norm. Given two sets $A$ and $B$, $A \subset B$ means that all elements of $A$ are included in $B$. Thus, $A$ and $B$ can also be equal.

## 2 PROBLEM SETTING AND MAIN RESULT

Given $c_1, \ldots, c_m \in \mathbb{R}^n$, with $c_i \neq c_j$ for $i \neq j$, we consider the multiobjective problem where each objective $f_i(x) = \frac{1}{2}\|x - c_i\|^2$ is a sphere function with optimum located in $c_i$. We additionally assume $p$ inequality constraints $g_i$ that are convex and continuous[1] and $q$ linear equality constraints $h_j$. More precisely, the problem reads as

$$\begin{aligned} &\text{minimize } \left(f_1(x) = \frac{1}{2}\|x - c_1\|^2, \ldots, f_m(x) = \frac{1}{2}\|x - c_m\|^2\right) \\ &\text{subject to } g_i(x) \leq 0, i = 1, \ldots, p \\ &\qquad h_j(x) = (a_j)^\top x + b_j = 0, j = 1, \ldots, q \end{aligned} \tag{2}$$

where $a_j \in \mathbb{R}^n$ are distinct vectors and $b_j \in \mathbb{R}$. We include in the above notation the possibility to set $p = 0$ or $q = 0$ (or both) which correspond to the cases of no inequality constraints or no equality constraints (or no constraints at all). As a particular case, the inequality constraints $g_i$ can be linear.

This problem is illustrated in Figures 2, 3, 4, 5 and 6 for varying numbers of constraints $p$, types of constraints (linear or spherical), and $m = 2$ and $m = 3$. The search space dimension is always $n = 2$ for visualization purposes. On the left plot, we display the problem in the search space and on the right plot in the objective space. In all figures, the objective functions' optima $c_i \in \mathbb{R}^n$ are displayed as black crosses, the unconstrained Pareto set $\mathrm{PS}^u$ (formally described above in (1) as the simplex between the $c_i$'s) is shown as (thin) gray points (or as a gray area in Figure 5). The Pareto front of the unconstrained problem is shown with the same gray color. In the background of the search space plots, we see the level sets of the objective functions as thin gray circles. The constraints are shown as (dashed and colored) lines with the infeasible space in the same color (but faded) which means the feasible set with respect to all constraints, introduced as $C$ below in (3), is shown in white. The Pareto sets and Pareto fronts are shown as thicker points, with colors indicating on which constraint boundary the Pareto optimal solutions lie (black points indicate that no constraint had an effect on the solution).

The feasible set $C$ is defined as the set of vectors of the search space $\mathbb{R}^n$ that satisfy all constraints. It corresponds to the white regions of the previously discussed plots (see also below for more detailed explanations). It is equal to the intersection of the feasible sets associated to each constraint. More precisely, consider $C_i = \{x \in \mathbb{R}^n, \text{ such that } g_i(x) \leq 0\}$ and $\overline{C}_j = \{x \in \mathbb{R}^n, \text{ such that } h_j(x) = 0\}$, the feasible set equals

$$\begin{aligned} C &= \{x \in \mathbb{R}^n, g_i(x) \leq 0, i = 1, \ldots, p, h_j(x) = 0, j = 1, \ldots q\} \\ &= \bigcap_{i=1}^p C_i \bigcap_{j=1}^q \overline{C}_j. \end{aligned} \tag{3}$$

Remark that if $p = 0$, then by convention $\bigcap_{i=1}^p C_i = \mathbb{R}^n$, and similarly if $q = 0$, $\bigcap_{j=1}^q \overline{C}_j = \mathbb{R}^n$. If the inequality constraints $g_i$ are defined on a closed convex subset of $\mathbb{R}^n$ denoted $D_i$, then each $C_i = \{x \in D_i, \text{ such that } g_i(x) \leq 0\}$ is a subset of $D_i$.

Denoting $f(x) = (f_1(x), \ldots, f_m(x))$, the vector valued function associated to the above problems, we can rewrite the optimization problem from (2) in a more compact way as

$$\min_{x \in C} f(x). \tag{4}$$

The feasible set $C$ for different instances of the double sphere problem with $n = 2$ variables is displayed in Figure 2 for the case of one linear inequality constraint, in Figure 3 for three different cases of two linear inequality constraints, in Figure 4 in the case of four linear inequality constraints, in Figure 5 for the 3-sphere problem with one linear constraint and in Figure 6 for the double sphere in the case of one linear and one spherical constraint. The feasible

[1]The functions $g_i$ can be defined on $D_i$, a closed convex subset of $\mathbb{R}^n$. The continuity is then assumed on $D_i$.

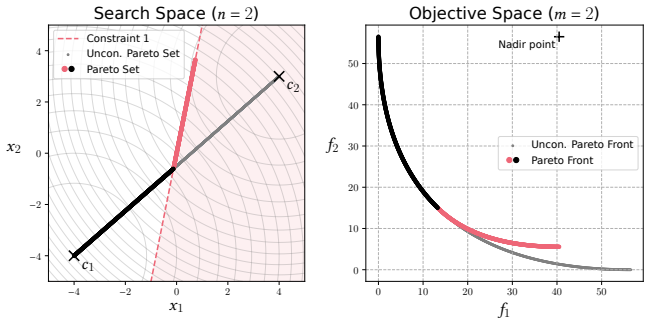


**Figure 2: Example problem with two variables, two spherical objectives and a single linear constraint.**

set corresponds in all cases to the white area (and boundary of the white area) which is indeed the intersection of the feasible sets associated to each constraint. We remark that this feasible set is a convex set. This property actually holds as soon as $g_i$ are convex and $h_j$ are linear. While this property is quite immediate, we formalize it in a lemma for the sake of clarity.

Lemma 2.1. *Assume a constrained problem with $p \geq 0$ inequality constraints $g_i, i = 1, \ldots, p$ that are convex and continuous and $q \geq 0$ linear equality constraints. Then the feasible set $C$ defined in* (3) *is closed and convex.*

Proof. Remark first that each $C_i = \{x \in \mathbb{R}^n, g_i(x) \leq 0\}$ is a sublevel set of the constraint $g_i$ and since we assume that the inequality constraints $g_i$ are convex, its sublevel sets are convex [3, Section 3.1.6]. Thus, $\{C_i, i = 1, \ldots, m\}$ are convex sets. In addition, the equality constraints are linear, so $\overline{C}_j = \{x, h_j(x) = 0\}$ is also a convex set. Overall, the feasible set $C$ is convex as the intersection of convex sets.

Each $C_i$ is also closed as $C_i = g_i^{-1}(]-\infty, 0])$ is the inverse image of the closed set $]-\infty, 0]$ by a continuous mapping. Similarly, $\overline{C}_j = h_j^{-1}(\{0\})$ are also closed sets. Then $C$ is closed as an intersection of closed sets. Overall, the set $C$ is closed and convex. □

A Pareto optimal solution is defined as a (feasible) solution that cannot be improved along one objective without deteriorating at least another:

*Definition 2.2 ([10, Definition 11.3]).* A vector $\bar{x}$ is called an efficient solution or Pareto optimal solution of a problem (4) if it is feasible, i.e., $\bar{x} \in C$ and if there is no $x \in C$ such that $f_i(x) \leq f_i(\bar{x})$ for all $i = 1, 2, \ldots, m$ and $f(x) \neq f(\bar{x})$.

When $C = \mathbb{R}^n$, we retrieve the classical definition of a Pareto optimal solution in the unconstrained case. We will refer to this set of Pareto optimal solutions of the unconstrained problem as the *unconstrained Pareto set* and denote it $\mathrm{PS}^u$. We also introduce the notion of weak Pareto optimality.

*Definition 2.3 ([10, Definition 11.5]).* A vector $\bar{x}$ is weakly efficient or a weakly Pareto optimal solution of a problem (4), if it is feasible and if there is no $x \in C$ with $f_i(x) < f_i(\bar{x})$ for all $i = 1, 2, \ldots, m$.

From the definition, we easily see that a Pareto optimal point is also weakly Pareto optimal but the reverse is not true in general.

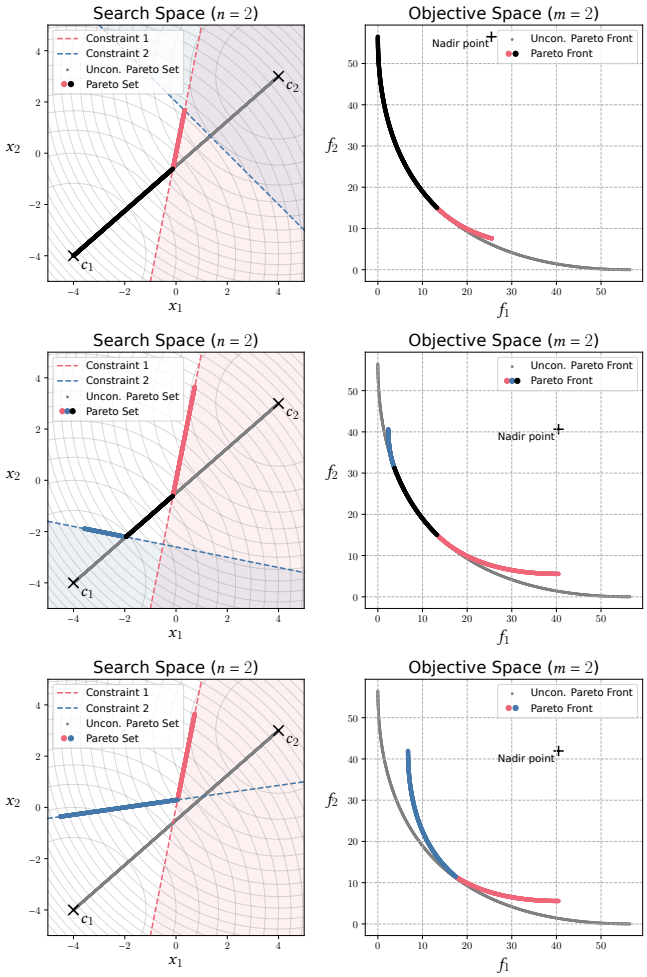


**Figure 3: Three example problems with two variables, two spherical objectives and two linear constraints.**

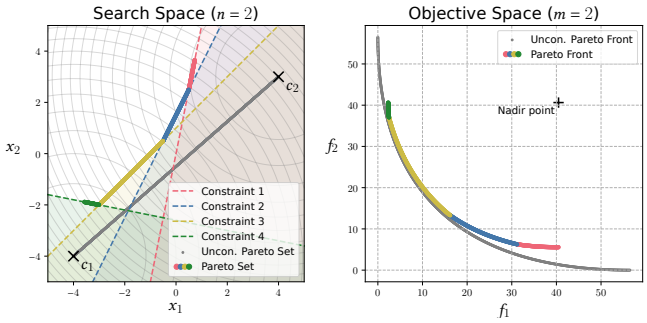


**Figure 4: Example problem with two variables, two spherical objectives and four linear constraints.**

In the case of two spherical objective functions, like in (2) with $m = 2$ and no constraints, the unconstrained Pareto set corresponds to the line segment between the single-objective optima $c_1$ and $c_2$

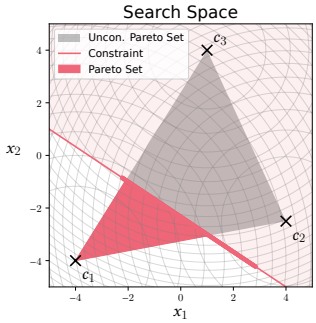


**Figure 5: Example problem with two variables, three spherical objectives and one linear constraint.**

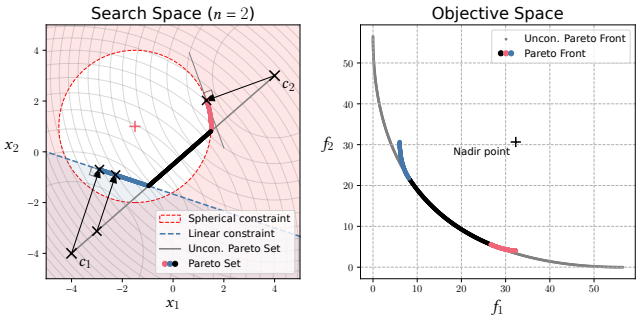


**Figure 6: Example problem with two variables, two spherical objectives and two constraints—one spherical (in red) and one linear (in blue). In addition to the unconstrained and constrained Pareto sets, the projection of three (unconstrained) Pareto optimal solutions (black crosses) onto the feasible domain are shown by black arrows.**

expressed formally in (1). This result is known, but we will provide a formal proof in Proposition 3.7 (see Section 3.2). Similarly, we will refer to the set of Pareto optimal solutions of the constrained problem (2) as the *constrained Pareto set* and denote it PS.

It is intuitive that if a point of the unconstrained Pareto set $x_t$ for some $t \in [0, 1]$ is included in the feasible domain, then it also belongs to the (constrained) Pareto set PS. The proof is also immediate: let $x_t \in \mathrm{PS}^u \cap C$; since by definition of $\mathrm{PS}^u$ we cannot find better solutions $x \in \mathbb{R}^n$ such that $f_i(x) \leq f_i(x_t)$ and $f(x) \neq f(x_t)$, then we can also not find any better solution in $C \subset \mathbb{R}^n$. This property and the proof sketched above is not restricted to a convex constraint, nor to the double sphere problem. We formalize it in the following lemma for an abstract multiobjective problem.

Lemma 2.4. *Consider a multiobjective problem $f = (f_1, \ldots, f_m)$ with inequality and equality constraints that define a feasible set $C$. Let $\mathrm{PS}^u$ and PS denote the unconstrained and constrained Pareto sets. Then, Pareto optimal points for the unconstrained problem that are feasible, belong to the Pareto set of the constrained problem. In other words,*

$$\mathrm{PS}^u \cap C \subset \mathrm{PS}.$$

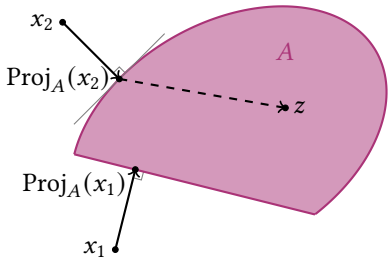


**Figure 7: Projection of $x_1$ and $x_2$ onto the closed convex set $A$. The projected points $P_A(x_i)$ achieve the minimal distance between $x_i$ and the set. The vector $x_i - P_A(x_i)$ is orthogonal to the tangent to the set and forms an angle which is larger than or equal to 90 degrees with any other vector $z - P_A(x_i)$, where $z$ belongs to $A$.**

Now that we know that the vectors of the unconstrained Pareto set that are feasible belong to PS, we can ask the questions:

- What happens to the Pareto optimal points that are infeasible?
- What are the other Pareto optimal points?

We will answer these two questions and prove that the Pareto set PS corresponds to the projection of the unconstrained Pareto set $\mathrm{PS}^u$ onto the feasible set. Prior to stating our main result, we explain what we intend by projection. Consider a vector $x \in \mathbb{R}^n$ and a set $A \subset \mathbb{R}^n$ assumed to be a closed convex set. We define the projection with respect to the Euclidean norm of $x$ onto $A$ as the unique point $y$ that achieves the minimal distance to any point in the set $A$

$$\|x - y\| = \min_{z \in A} \|x - z\|.$$

The existence and unicity of $y$ is a consequence of the projection theorem stated in Theorem 3.4 (see Section 3.1). Given $x$, the projection vector $y$ of $x$ onto $A$ is denoted

$$y = \mathrm{Proj}_A(x).$$

The projection operator is illustrated in Figure 7. Remark that if $x \in A$, then $\mathrm{Proj}_A(x) = x$.

Theorem 2.5. *Consider the $m$-objective spherical problem (2), with convex constraints ($g_i$ are convex and continuous and $h_j$ are linear). Let $C$ be its associated feasible set defined in (3). Assume that $C$ is non-empty, then the Pareto set is equal to the projection of $\mathrm{PS}^u$ onto the (closed convex) feasible set $C$:*

$$\mathrm{PS} = \{\mathrm{Proj}_C(x), x \in \mathrm{PS}^u\} = \left(\mathrm{PS}^u \cap C\right) \cup \{\mathrm{Proj}_C(x), x \in \mathrm{PS}^u \cap C^c\}$$

*where $C^c$ denotes the complementary set of $C$.*

We illustrate the projections of the previous theorem with respect to the Euclidean norm onto a convex set in Figure 6 for the double-sphere problem with one spherical convex constraint (points are feasible w.r.t. this constraint if they are within or on the circle) and one linear constraint. The unconstrained Pareto set $\mathrm{PS}^u$ is the line segment between $c_1$ and $c_2$ depicted in gray. The feasible set $C$ corresponds to the white area plus its boundary. The constrained Pareto set PS is composed of three parts respectively depicted with thick lines in black, blue and red. The black part corresponds to the

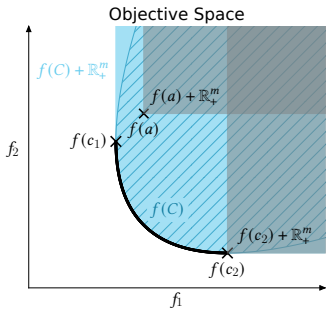


**Figure 8: An illustration of the feasible objective space $f(C)$ (hatched in blue), its extension towards $f(C)+\mathbb{R}^2_+$ (light blue), and the same extensions $f(\{a\})+\mathbb{R}^2_+$ and $f(\{c_2\})+\mathbb{R}^2_+$ for two single solutions $a, c_2 \in \mathbb{R}^n$ (in light gray).**

points that belong to $\mathrm{PS}^u$ and are feasible. The blue part corresponds to the projection of the unconstrained Pareto set being infeasible due to the linear constraint to the feasible set. We illustrate in particular the projection of $c_1$ and another point using black arrows. Lastly, the red part corresponds to the projection of the infeasible unconstrained Pareto set to the feasible set where the infeasibility comes from the spherical constraint.

## 3 PROOF OF THE MAIN RESULT

The proof of our main theorem (Theorem 2.5) is an application of two classical results stemming from convex optimization. First, the connection between the Pareto set and the optima of the linear scalarization of the objectives. Second, the projection theorem onto non-empty closed convex sets. In Section 3.1, we first review the relevant definitions and theorems. We then provide some preliminary technical results in Section 3.2. Finally, we present the detailed proof in Section 3.3.

### 3.1 Background

Given a multiobjective problem $\min_{x\in C} f(x)$ for a non empty set $C$ we denote by $f(C)+\mathbb{R}^m_+$ [10, Page 299] the set

$$f(C)+\mathbb{R}^m_+ := \{y \in \mathbb{R}^m, y_i \geq f_i(x) \text{ for some } x \in C \text{ and all } i \in \{1,\dots,m\}\}. \quad (5)$$

Figure 8 illustrates the sets $f(C)$ and $f(C)+\mathbb{R}^m_+$ for the case of $m=2$ spherical objective functions and no constraints, as well as for two exemplary solutions $a, c_2 \in \mathbb{R}^n$, mapped to the objective vectors $f(\{a\})$ and $f(\{c_2\})$, the sets $f(\{a\})+\mathbb{R}^2_+$ and $f(\{c_2\})+\mathbb{R}^2_+$ respectively.

If the functions $f_i$ are convex and the set $C$ is convex, then the set $f(C)+\mathbb{R}^m_+$ is convex [3, Page 180]. We formalize this simple result and provide a proof in the appendix for the sake of completeness.

Lemma 3.1. *Assume that the objective functions $f_i$, $i=1,2,\dots,m$, are convex and the set $C$ is a convex subset of $\mathbb{R}^n$. Then the set $f(C)+\mathbb{R}^m_+$ is a convex subset of $\mathbb{R}^m$.*

We have introduced the notion of Pareto optimality and weak Pareto optimality. While in general not all weakly Pareto optimal points are Pareto optimal, in the case where the objectives $f_i$ are strictly convex, weakly Pareto optimal points and Pareto optimal points coincide as stated in the next lemma.

Lemma 3.2 ([1, Lemma 1.3]). *If all objectives $f_i$ are continuous and strictly convex, then a vector is Pareto optimal if and only if it is weakly Pareto optimal.*

Under the assumption that the set $f(C)+\mathbb{R}^m_+$ is convex, we can connect the weakly Pareto optimal solutions of $\min_{x\in C} f(x)$ with the optima of the scalarized single-objective problems. More precisely, the following result holds.

Theorem 3.3 ([10, Table 11.5, Page 302]). *Consider a multiobjective problem $\min_{x\in C} f(x)$ with $f=(f_1,\dots,f_m)$ and $C$ a non-empty set. Assume $f(C)+\mathbb{R}^m_+$ is a convex set. A vector $\bar{x}$ is a weakly Pareto optimal solution of the multiobjective problem if and only if there exist $t_1,\dots,t_m \geq 0$ with at least one $t_i > 0$ such that $\bar{x} \in \operatorname{argmin}_{x\in C} \sum_{i=1}^m t_i f_i(x)$.*[2]

We now present another useful result, which corresponds to the Hilbert projection theorem [8, Section 3.1], formulated here for the finite dimensional search space $\mathbb{R}^n$ that is relevant to our case and illustrated in Figure 7.

Theorem 3.4. *Consider a norm $\|.\|$ deriving from an inner product $\langle .,. \rangle$ in $\mathbb{R}^n$ and $C \subset \mathbb{R}^n$ a non-empty closed convex set. For every $x \in \mathbb{R}^n$, there exists a unique $y \in C$ such that*

$$\|x-y\| = \inf_{z\in C} \|x-z\|.$$

*The vector $y$ is called the projection of $x$ onto $C$ and denoted $y = \mathrm{Proj}_C(x)$. In addition, $y$ is equivalently characterized by*

$$\langle x-y, z-y\rangle \leq 0 \qquad \text{for all } z \in C. \quad (6)$$

### 3.2 Preliminary results

We consider quadratic functions on $\mathbb{R}^n$ defined as $f(x) = \frac{1}{2}x^\top Ax + b^\top x + c$ with $A \succeq 0$, i.e. $A$ is symmetric positive, $b \in \mathbb{R}^n$ and $c \in \mathbb{R}$. It is a classical result that quadratic functions are convex if $A \succeq 0$ (in which case we talk about convex-quadratic functions) and strictly convex if $A$ is additionally definite (i.e. $x=0$ if and only if $x^\top Ax = 0$). We denote $A \succ 0$ when $A$ is symmetric positive definite. Given $A \succ 0$, it can be easily seen that the Hessian matrix of $f$ is constant and equal to $A = \nabla^2 f(x)$ for all $x$. We will use in the sequel that a convex-quadratic function can be parametrized entirely by its Hessian matrix and optimum. We formalize the result in the next lemma. The proof is straightforward from standard calculus.

Lemma 3.5. *Consider a convex-quadratic function $f(x) = \frac{1}{2}x^\top Ax + b^\top x + c$ with $A \succ 0$ a symmetric definite positive matrix, $a \in \mathbb{R}^n$ and $b \in \mathbb{R}$. Then $f$ can be written in factorized form as*

$$f(x) = \frac{1}{2}(x-x^*)^\top A(x-x^*) + c - \frac{1}{2}b^\top A^{-1}b$$

*where $x^*$ is the minimizer of $f$ which is given as $x^* = -A^{-1}b$. It is thus entirely determined by its Hessian matrix $A$ and optimum.*

[2] The same reference [10, Table 11.5, Page 302] connects Pareto optimal points to the optima of scalarized functions in the following way: If $\bar{x}$ is a Pareto optimal solution of the multiobjective problem, then there exist $t_1,\dots,t_m \geq 0$ with at least one $t_i > 0$ such that $\bar{x} \in \operatorname{argmin}_{x\in C} \sum_{i=1}^m t_i f_i(x)$. Conversely, let $t_1,\dots,t_m > 0$ be $m$ strictly positive scalars, and let $\bar{x} \in \operatorname{argmin}_{x\in C} \sum_{i=1}^m t_i f_i(x)$, then $\bar{x}$ is Pareto optimal for the multiobjective problem.

*Conversely, every function* $\frac{1}{2}(x-\bar{x}^\star)^\top B(x-\bar{x}^\star)$ *with* $B \succeq 0$ *is convex-quadratic with developed form* $f(x) = \frac{1}{2}x^\top Bx - (B\bar{x}^\star)^\top x + \frac{1}{2}\bar{x}^\star B\bar{x}^\star$.

We show next that a convex combination of convex-quadratic functions is convex-quadratic and identify its Hessian and optimum.

Lemma 3.6. *Consider m strictly convex quadratic functions* $f_i(x) = \frac{1}{2}(x-c_i)^\top H_i(x-c_i)$ *with* $H_i \succ 0$. *Let* $t_1,\ldots,t_m \geq 0$ *and* $\sum_i t_i = 1$ *and consider the convex-combination of the m objectives* $\mathcal{F}_t(x) = t_1 f_1(x) + \ldots + t_m f_m(x)$. *Then* $x \mapsto \mathcal{F}_t(x)$ *is also strictly convex-quadratic function with Hessian matrix* $H_t = t_1H_1 + \ldots + t_mH_m$ *and optimum* $c_t = H_t^{-1}(\sum_i t_i H_i c_i)$, *i.e.*

$$\mathcal{F}_t(x) = \sum_{i=1}^{m} t_i f_i(x) = \frac{1}{2}(x-c_t)^\top H_t (x-c_t).$$

Proof. Given $t_1,\ldots,t_m \geq 0$ and $\sum_i t_i = 1$, developing $x \mapsto \sum t_i f_i(x)$, we find that the function is composed of quadratic terms in the coordinates of $x$, linear terms and constant terms, thus it is a quadratic function with quadratic term equal to $\frac{1}{2}x^\top H_t x$. This identifies that the Hessian matrix of $\mathcal{F}_t$ equals $H_t$.

Since $H_i \succ 0$ and $t_i \geq 0$ with at least one $t_i$ strictly positive, then $\sum t_i H_i \succ 0$. Since $H_t \succ 0$, $x \mapsto \sum t_i f_i(x)$ is strictly convex quadratic. To determine the optimum of the convex quadratic function and thus its factorized form (see Lemma 3.5), we can compute the gradient of $\mathcal{F}_t(x) = \sum t_i f_i(x)$. By linearity, $\nabla\mathcal{F}_t(x) = \sum_i t_i \nabla f_i(x) = \sum_i t_i H_i(x-c_i)$. Hence the optimum $c_t$ of $\mathcal{F}_t$ satisfies $\nabla\mathcal{F}_t(c_t) = 0$, i.e. $\sum_i t_i H_i(c_t - c_i) = 0$, i.e. $H_t c_t = \sum t_i H_i c_i$, i.e. $c_t = H_t^{-1}(\sum_i t_i H_i c_i)$. □

We formalize and prove in the next proposition that the Pareto set of the unconstrained $m$-sphere problem is the convex hull of the centers of the spheres. This result is known, however, the proof of our main result follows similar steps. We, therefore, provide a detailed proof.

Proposition 3.7. *Consider the m objective sphere problem* $(f_1(x) = \frac{1}{2}\|x-c_1\|^2, \ldots, f_m(x) = \frac{1}{2}\|x-c_m\|^2)$ *where the centers* $c_i$ *are in* $\mathbb{R}^n$. *The Pareto set of this unconstrained problem is composed of the optima of the scalarized (single)-objective functions* $\sum t_i f_i(x)$ *for* $t_i \geq 0$ *and* $\sum_i t_i = 1$. *Each such function* $x \mapsto \sum t_i f_i(x)$ *is also a sphere function with the optimum being the corresponding convex combination of the sphere centers. Formally, the Pareto set is composed of the optima of*

$$\left\{ x \mapsto \sum t_i f_i(x) = \frac{1}{2}\|x-c_t\|^2, t_i \geq 0 \text{ and } \sum_i t_i = 1 \right\}$$

*where given* $(t_1,\ldots,t_m)$ *with* $\sum t_i = 1$ *we denote* $c_t := \sum_i t_i c_i$. *Hence, the Pareto set is the convex hull of the sphere centers* $c_1,\ldots,c_m$, *i.e.*

$$\mathrm{PS}^u = \left\{ t_1c_1 + \ldots + t_mc_m, t_i \geq 0, \sum t_i = 1 \right\}.$$

Proof. Let $\bar{x} \in \mathrm{PS}^u$ be a Pareto optimal solution which is also weakly Pareto optimal. Since $f_i$ are convex, and $\mathbb{R}^n$ is convex, by Lemma 3.1, $f(\mathbb{R}^n) + \mathbb{R}^m_+$ is convex and the assumption of Theorem 3.3 is satisfied. We therefore know that $\bar{x}$ is the minimizer of $x \in \mathbb{R}^n \mapsto t'_i f_i(x)$ for $t'_i \geq 0$ with at least one $t'_i$ strictly positive. Since $\sum_i t'_i > 0$ and the minimizer of a function is unchanged, if we scale the function by a positive factor, $\bar{x}$ is also a minimizer of $x \in \mathbb{R}^n \mapsto \sum_i t'_i/(\sum_j t'_j) f_i(x)$. Denote $t_i = t'_i/(\sum_j t'_j) \in [0,1]$, remark that $\sum t_i = 1$ such that $\bar{x}$ is the minimizer of $x \to \sum t_i f_i(x)$. According to Lemma 3.6, plugging $H_i = I_d$, then $\sum t_i f_i(x) = \frac{1}{2}\|x-c_t\|^2$ where $c_t = \sum t_i c_i$. We have thus proven that $\mathrm{PS}^u \subset \{t_1c_1 + \ldots + t_mc_m, t_i \geq 0, \sum t_i = 1\}$.

Conversely consider the minimizer of the convex combination of $f_i, x \mapsto \sum t_i f_i(x)$ for $t_i \geq 0$ with $\sum t_i = 1$. According to Theorem 3.3, this minimizer is weakly Pareto optimal. By strict convexity of the objectives $f_i$ we know that a weakly Pareto optimal point is Pareto optimal and thus, $\{t_1c_1 + \ldots + t_mc_m, t_i \geq 0, \sum t_i = 1\} \subset \mathrm{PS}^u$.

□

## 3.3 Proof of Theorem 2.5

According to Lemma 2.1, the feasible set $C$ is closed and convex. In addition, we assume it is non-empty and thus satisfies the assumption needed for the projection Theorem 3.4.

Each objective function $f_i$ is convex (even strictly convex) and thus, according to Lemma 3.1, since $C$ is convex, $f(C)+\mathbb{R}^2_+$ is convex. Thus, according to Theorem 3.3, $\bar{x}$ is weakly Pareto optimal for (2) if and only if there exist $t'_1 \geq 0, \ldots, t'_m \geq 0$ and at least one non-zero $t'_i$ such that $\bar{x} \in \mathrm{argmin}_{x\in C} t'_1 f_1(x) + \ldots + t'_m f_m(x)$.

Dividing by $\sum_i t'_i$ and calling $t_i = t'_i/\sum_i t'_i$, we have that $t_i \geq 0$ and $\sum_i t_i = 1$ as well as

$$\begin{aligned} \bar{x} \in \mathrm{argmin}_{x\in C} \sum_i t_i f_i(x) &= \mathrm{argmin}_{x\in C} \frac{1}{2}\|x-c_t\|^2 \\ &= \mathrm{argmin}_{x\in C}\|x-c_t\|^2 = \mathrm{argmin}_{x\in C}\|c_t - x\| \end{aligned} \tag{7}$$

with $c_t = \sum t_i c_i$ where we have used Lemma 3.6 to identify that $\sum t_i f_i(x) = \frac{1}{2}\|x-c_t\|^2$.

Scrutinizing (7), we see that $\bar{x}$ corresponds to the unique projection of $c_t$ onto the closed non-empty convex set $C$. In addition, we have proven in Proposition 3.7 that $c_t = \sum t_i c_i$ with $t_i \geq 0$ are Pareto optimal for the unconstrained problem.

Overall, we have shown that $\bar{x}$ is weakly Pareto optimal, if and only if it is the unique projection of a vector $c_t = \sum t_i c_i$ with $t_i \geq 0$ and $\sum t_i = 1$ of the unconstrained Pareto set. Hence, since $f_i$ are strictly convex and weakly Pareto optimal points and Pareto optimal points coincide, we have $\mathrm{PS} = \{\mathrm{Proj}_C(x), x = \sum t_i c_i, t_i \geq 0 \text{ and } \sum t_i = 1\}$.

Overall, we have shown that $\mathrm{PS} = \{\mathrm{Proj}_C(x), x \in \mathrm{PS}^u\}$. Using Lemma 2.4, we can decompose PS as

$$\mathrm{PS} = \left(\mathrm{PS}^u \cap C\right) \cup \{\mathrm{Proj}_C(x), x \in \mathrm{PS}^u \cap C^c\}.$$

# 4 A BENCHMARKING PERSPECTIVE

When assessing the performance of multiobjective algorithms, we typically report quality indicator values over time. Many of these indicators inherently depend on the Pareto set and/or front of the benchmarked problem or their approximations. Even when this is not the case, knowing the Pareto set and front allows us to display relative performance to the (approximated) optimal quality indicator value, which is valuable when assessing the absolute performance of an algorithm. It provides insights into questions such as: "How close to the actual optimum can we optimize?" and "How fast does the algorithm approximate the optimum with a given precision?"

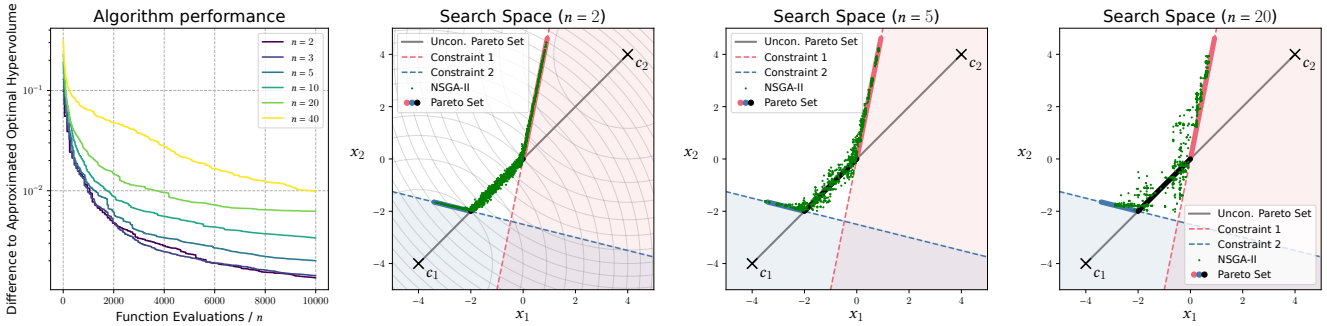


**Figure 9: NSGA-II performance on problems with two spherical objectives, two linear constraints and 2, 3, 5, 10, 20 or 40 variables with respect to the hypervolume difference to the optimal hypervolume over time, measured as the number of function evaluations divided by dimension $n$ (left). The other three plots show the projections of all non-dominated solutions found by NSGA-II in the entire run onto the $x_1$-$x_2$ plane (green dots) for three chosen number of variables: 2, 5, and 20.**

## 4.1 Computing the Pareto Set and Front

In the case of the $m$-objective sphere function with linear constraints, since the Pareto set corresponds to the set of solutions of the scalarized problem $x \to \sum t_i f_i(x)$ for $t_i \geq 0$ with $\sum t_i = 1$ with linear constraints, we can compute the Pareto sets numerically by fixing $t_i \geq 0$ with $\sum t_i = 1$ and using the KKT conditions on the single-objective constraint problem. Since Slaters's qualification condition holds, the KKT conditions are both necessary and sufficient for optimality. The stationary condition reduces to a set of linear equations.

## 4.2 Example Performance of NSGA-II

To demonstrate how the knowledge of the Pareto set can be exploited to examine the performance of a multiobjective evolutionary algorithm on the investigated problems, we choose a family of problems with two spherical objectives and two linear constraints, and the Non-Dominated Sorting Genetic Algorithm II (NSGA-II) [5]. The problems in this experiment are parameterized as follows:

- The centers of the two spherical objectives are located at points $c_1 = (-4, \ldots, -4)$ and $c_2 = (4, \ldots, 4)$.
- Each of the two constraint planes is defined by a point on the plane $P$ and the normal vector $n$ with $P_1 = (0, \ldots, 0)$ and $n_1 = (5, -1, 0, \ldots, 0)$ for the first constraint, and $P_2 = (-2, \ldots, -2)$ and $n_2 = (-1, -4, 0, \ldots, 0)$ for the second constraint. For visualization purposes, the constraint planes are chosen so that they are always perpendicular to the $x_1$-$x_2$ plane (their normal vector coordinates in dimensions larger than two are always zero).

We instantiate this problem in six different dimensions, 2, 3, 5, 10, 20, and 40. We use the implementation of NSGA-II from the `pymoo` Python library [2] with the population size of 100 and the limit of $10^4 n$ function evaluations. Remaining parameters are kept at their default values. The results of single runs of NSGA-II are shown in Figure 9. The left-most plot displays the hypervolume indicator[3] difference between a fixed-size approximation of the true Pareto front[4] and the best-so-far solutions found by NSGA-II over time (in terms of number of function evaluations, normalized by problem dimension). The other three plots show the projections of all non-dominated solutions found by NSGA-II (within a single run) onto the first two variables when the problem dimension $n$ equals 2, 5 and 20, respectively.

We observe that NSGA-II finds solutions along the constrained Pareto set, which become better and better (in hypervolume) over time. We also observe that the NSGA-II performance is, as expected, degrading with increasing dimension: both the hypervolume differences as well as the visually seen distances to the Pareto set are larger for higher dimensions. However, the degradation is less apparent in the objective space (not pictured). The knowledge of the constrained Pareto set further allows to distinguish different behaviors of NSGA-II along it: while on the outer parts of the Pareto set, the solutions found by NSGA-II are restricted to one side of the Pareto set due to the constraints, the absence of constraint boundaries near the inner part of the Pareto set results in solutions found on both sides.

## 5 CONCLUSION

In this paper, we analyzed the $m$-sphere multiobjective problem with convex constraints. We proved the simple result that the (constrained) Pareto set corresponds to the orthogonal projection of the (well-identified) unconstrained Pareto set onto the feasible set. We visualized this Pareto set in the search space and objective space in different scenarios: with two and three objectives, with different numbers of linear constraints plus a spherical one. We illustrated how NSGA-II approximates this Pareto set when varying the problem dimension for the case of two constraints. This work is an illustration of how theory, when addressing the right questions, can help understand fundamental properties and accompany the construction of test problems. Our theoretical insight has direct practical implications for benchmarking: the analytical/numerical knowledge of the Pareto set and Pareto front of the investigated

[3]The hypervolume indicator uses the nadir point as the reference point and is normalized so that the ideal point corresponds to $(0, 0)$ and the nadir point to $(1, 1)$.

[4]To obtain the Pareto front approximation, $10^6$ equidistant points from the unconstrained Pareto set were first projected onto the feasible space and then evaluated.

problems enables the analysis of optimization algorithms' convergence towards the true optimum. It also allows the use of quality indicators that would not be applicable if the Pareto set and Pareto front were unknown. Furthermore, it highlights the important role of visualization in gaining insights and supporting algorithm design.

## ACKNOWLEDGMENTS

The first author would like to thank Armen Chahmirian, Ilyas Glaib and Gautier Vantalon for their feedback on the first version of this paper which helped to greatly simplify the proofs. We acknowledge financial support from the Slovenian Research and Innovation Agency (research core funding No. P2-0209 and projects No. N2-0254 "Constrained Multiobjective Optimization Based on Problem Landscape Analysis" and GC-0001 "Artificial Intelligence for Science"). This paper stems from a collaboration established within COST Action CA22137 "Randomised Optimisation Algorithms Research Network" (ROAR-NET), supported by COST (European Cooperation in Science and Technology).

## A ADDITIONAL PROOFS

### Proof of Lemma 3.1

Proof. Let $y$ and $\bar{y}$ be element of $f(C)+\mathbb{R}^m_+$. Let $\lambda \in [0,1]$, we will prove that $\lambda y + (1-\lambda)\bar{y}$ belongs to $f(C)+\mathbb{R}^m_+$. This will prove the convexity of $f(C)+\mathbb{R}^m_+$. Since $y \in f(C)+\mathbb{R}^m_+$, there exist $s \in C$ and $z \in \mathbb{R}^m_+$ such that $y = f(s)+z$. Similarly, there exist $\bar{s} \in S$ and $\bar{z} \in \mathbb{R}^m_+$ such that $\bar{y} = f(\bar{s})+\bar{z}$. Then $\lambda y + (1-\lambda)\bar{y} = \lambda f(s) + (1-\lambda)f(\bar{s}) + \lambda z + (1-\lambda)\bar{z}$. The coordinate $i$ of the vector $\lambda f(s)+(1-\lambda)f(\bar{s})$ equals $\lambda f_i(s) + (1-\lambda)f_i(\bar{s})$. By convexity of $f_i$, it is larger or equal to $f_i(\lambda s + (1-\lambda)\bar{s})$. Hence each coordinate of $\lambda f(s)+(1-\lambda)f(\bar{s})$ is larger or equal to the coordinates of $f(\lambda s+(1-\lambda)\bar{s})$. Hence, there exists $\tilde{z} \in \mathbb{R}^m_+$ such that $\lambda f(s)+(1-\lambda)f(\bar{s}) = f(\lambda s+(1-\lambda)\bar{s})+\tilde{z}$ (the coordinate $i$ of $\tilde{z}$ equal $\lambda f_i(s) + (1-\lambda)f_i(\bar{s}) - f_i(\lambda s+(1-\lambda)\bar{s}) \geq 0$). Since $S$ is convex, $\lambda s + (1-\lambda)\bar{s}$ belongs to $S$ and thus

$$\lambda f(s) + (1-\lambda)f(\bar{s}) = f(\tilde{s}) + \tilde{z}.$$

We have thus shown that $\lambda y + (1-\lambda)\bar{y} = f(\tilde{s}) + \tilde{z} + \lambda z + (1-\lambda)\bar{z}$. Since $\tilde{z}, z, \bar{z}$ belong to $\mathbb{R}^m_+$, then $\tilde{z} + \lambda z + (1-\lambda)\bar{z}$ belong to $\mathbb{R}^m_+$ (we add non-negative coordinates, so we preserve the non-negativity). Hence $\lambda y + (1-\lambda)\bar{y} \in f(C)+\mathbb{R}^m_+$. □

## B ADDITIONAL MATERIAL

We include some interesting complementary definitions and results, although not needed for the proof of the main result. We recall the definition of *Pareto critical points* in the case where the objectives $f_i$ are differentiable[5].

*Definition B.1.* A vector $\bar{x} \in \mathbb{R}^n$ is Pareto critical if and only if $\max_{i=1,\ldots,m} \nabla f_i(\bar{x})^\top v \geq 0$ for all $v \in \mathbb{R}^n$.

It follows directly from this definition, that a solution $x \in \mathbb{R}^n$ is non-critical if there exists a direction $v \in \mathbb{R}^n$ such that for all $i = 1, \ldots, m$ we have $\nabla f_i(x)v < 0$ (in other words that we can follow the descent direction $v$ towards better values in all objectives).

[5]By differentiable we assume differentiable in the sense of Frechet, while we only need directional derivatives (which exist for convex functions) to define Pareto critical points (see [17]).

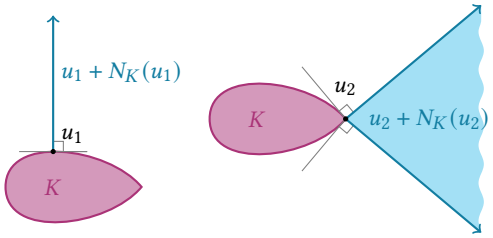


**Figure 10: Normal cones at $u_1$ and $u_2$ to a convex set $K$.**

When the objectives are strictly convex, then Pareto critical points are also Pareto optimal.

Lemma B.2 ([17]). *Consider an unconstrained multiobjective problem where the objectives $f_i$ are differentiable. If every objective $f_i$ is strictly convex, then every Pareto critical point is also Pareto optimal.*

The definition of Pareto critical points can be generalized to constrained multiobjective problems using the notion of a normal cone to a convex set that we recall below.

*Definition B.3 (Normal cone [14, Page 15]).* Consider $K$ a non-empty closed convex set. The normal cone to $K$ at $u \in K$ is defined as $N_K(u) = \{v \in \mathbb{R}^n, v^\top(z-u) \leq 0 \text{ for all } z \in K\}$.

The notion of normal cone is illustrated in Figure 10. Critical points of a constrained multiobjective problem are defined for differentiable convex objectives as follows.

*Definition B.4 ([1, Definition 1.2]).* Given a closed convex feasible set $C$, we say that $\bar{x} \in C$ is Pareto critical for the constrained multiobjective problem $\min_{x \in C} f(x)$ where $f$ is convex and differentiable, if there exist $t_1, \ldots, t_m \geq 0$ with $\sum t_i = 1$ such that

$$-\sum t_i \nabla f_i(\bar{x}) \in N_C(\bar{x}).$$

The previous definition can be extended to non-differentiable functions, via the notion of subdifferential (see [1]).

Similarly to Lemma B.2, when the objectives are strictly convex, Pareto optimal points and Pareto critical points coincide.

Lemma B.5 ([1, Lemma 1.3]). *If all objectives $f_i$ are strictly convex and differentiable and the feasible set $C$ is a closed convex non-empty set, then there is equivalence between Pareto optimal points, Pareto critical points and weakly Pareto optimal points.*

Lemma B.6. *Consider a point of the unconstrained Pareto set $x = \sum t_i c_i$ with $t_i \geq 0$, $\sum t_i = 1$. Consider $y = \mathrm{Proj}_C(x)$ the unique projection of $x$ onto the feasible set $C$. Then $-\sum t_i \nabla f_i(y) \in N_C(y)$. In other words, $y$ is Pareto critical in the sense of Definition B.4 for the constrained problem.*

Proof. Let $x = \sum t_i c_i$ with $t_i \geq 0$, $\sum t_i = 1$ Let $y = \mathrm{Proj}_C(x)$. By definition of the normal cone in $y$, $-\sum t_i \nabla f_i(y) \in N_C(y)$ if $\langle -\sum t_i \nabla f_i(y), z-y \rangle \leq$ for all $z \in C$. This is thus the property that we need to prove. By the characterization of the projection given in Theorem 3.4, for all $z \in C$

$$\langle x-y, z-y \rangle \leq 0. \tag{8}$$

Yet, since $\nabla f_i(y) = y - c_i$, then $-\sum t_i \nabla f_i(y) = -\sum t_i(y-c_i) = -y + x$ since $\sum t_i = 1$ and $\sum t_i c_i = x$. Therefore, (8) is equivalent to $\langle -\sum t_i \nabla f_i(y), z-y \rangle \leq 0$, and thus $-\sum t_i \nabla f_i(y) \in N_C(y)$. □

# REFERENCES


[1] Hedy Attouch, Guillaume Garrigos, and Xavier Goudou. 2015. A dynamic gradient approach to Pareto optimization with nonsmooth convex objective functions. *J. Math. Anal. Appl.* 422, 1 (2015), 741–771.

[2] J. Blank and K. Deb. 2020. pymoo: Multi-Objective Optimization in Python. *IEEE Access* 8 (2020), 89497–89509.

[3] S. Boyd and L. Vandenberghe. 2004. *Convex optimization*. Cambridge University Press, The Edinburgh Building, Cambridge, CB2 8RU, UK.

[4] Dimo Brockhoff, Anne Auger, Nikolaus Hansen, and Tea Tušar. 2022. Using well-understood single-objective functions in multiobjective black-box optimization test suites. *Evolutionary Computation* 30, 2 (2022), 165–193.

[5] Kalyanmoy Deb, Samir Agrawal, Amrit Pratap, and T. Meyarivan. 2002. A fast and elitist multiobjective genetic algorithm: NSGA-II. *IEEE Transactions on Evolutionary Computation* 6, 2 (2002), 182–197. https://doi.org/10.1109/4235.996017

[6] Zhun Fan, Wenji Li, Xinye Cai, Hui Li, Caimin Wei, Qingfu Zhang, Kalyanmoy Deb, and Erik Goodman. 2020. Difficulty adjustable and scalable constrained multiobjective test problem toolkit. *Evolutionary computation* 28, 3 (2020), 339–378.

[7] Nikolaus Hansen, Anne Auger, Raymond Ros, Olaf Mersmann, Tea Tušar, and Dimo Brockhoff. 2021. COCO: A platform for comparing continuous optimizers in a black-box setting. *Optimization Methods and Software* 36, 1 (2021), 114–144.

[8] Jean-Baptiste Hiriart-Urruty and Claude Lemaréchal. 2004. *Fundamentals of convex analysis*. Springer, Berlin, Heidelberg.

[9] Christian Igel, Nikolaus Hansen, and Stefan Roth. 2007. Covariance matrix adaptation for multi-objective optimization. *Evolutionary computation* 15, 1 (2007), 1–28.

[10] Johannes Jahn. 2009. *Vector optimization*. Springer, Berlin, Heidelberg. https://doi.org/10.1007/978-3-642-17005-8

[11] Jing Liang, Xuanxuan Ban, Kunjie Yu, Boyang Qu, Kangjia Qiao, Caitong Yue, Ke Chen, and Kay Chen Tan. 2022. A survey on evolutionary constrained multiobjective optimization. *IEEE Transactions on Evolutionary Computation* 27, 2 (2022), 201–221.

[12] Zhi-Zhong Liu and Yong Wang. 2019. Handling constrained multiobjective optimization problems with constraints in both the decision and objective spaces. *IEEE Transactions on Evolutionary Computation* 23, 5 (2019), 870–884.

[13] Yang Nan, Hisao Ishibuchi, Tianye Shu, and Ke Shang. 2024. Analysis of real-world constrained multi-objective problems and performance comparison of multi-objective algorithms. In *Genetic and Evolutionary Computation Conference (GECCO 2024)*. ACM, New York, NY, 576–584.

[14] R. Tyrrell Rockafellar. 1970. *Convex analysis*. Princeton University Press, Princeton, N. J.

[15] Amit Saha and Tapabrata Ray. 2012. Equality constrained multi-objective optimization. In *Congress on Evolutionary Computation (CEC 2012)*. IEEE, Piscataway, NJ, 1–7.

[16] J David Schaffer. 1985. Multiple objective optimization with vector evaluated genetic algorithms. In *Proceedings of the 1st International Conference on Genetic Algorithms*. Lawrence Erlbaum Associates, Hillsdale, NJ, 93–100.

[17] Hiroki Tanabe, Ellen H Fukuda, and Nobuo Yamashita. 2019. Proximal gradient methods for multiobjective optimization and their applications. *Computational Optimization and Applications* 72 (2019), 339–361.

[18] Yuren Zhou, Yi Xiang, and Xiaoyu He. 2020. Constrained multiobjective optimization: Test problem construction and performance evaluations. *IEEE Transactions on Evolutionary Computation* 25, 1 (2020), 172–186.